HHS Public Access

Author manuscript

Ann Biomed Eng. Author manuscript; available in PMC 2018 February 01.

Published in final edited form as:

Ann Biomed Eng. 2017 February ; 45(2): 439–451. doi:10.1007/s10439-016-1605-7.

Implantation of a Tissue-Engineered Tubular Heart Valve in Growing Lambs

Jay Reimer[1], **Zeeshan Syedain**[1], **Bee Haynie**, **Matthew Lahti**[3], **James Berry**[3], and **Robert Tranquillo**[1,2]

[1] Department of Biomedical Engineering, University of Minnesota

[2] Department of Chemical Engineering and Material Science, University of Minnesota

[3] Experimental Surgical Services, University of Minnesota

Abstract

Current pediatric heart valve replacement options are suboptimal because they are incapable of somatic growth. Thus, children typically have multiple surgeries to replace outgrown valves. In this study, we present the *in vivo* function and growth potential of our tissue-engineered pediatric tubular valve. The valves were fabricated by sewing two decellularized engineered tissue tubes together in a prescribed pattern using degradable sutures and subsequently implanted into the main pulmonary artery of growing lambs.

Valve function was monitored using periodic ultrasounds after implantation throughout the duration of the study. The valves functioned well up to eight weeks, four weeks beyond the suture strength half-life, after which their insufficiency index worsened. Histology from the explanted valves revealed extensive host cell invasion occurred within the engineered root and commenced from the leaflet surfaces. These cells expressed multiple phenotypes, including endothelial, and deposited elastin and collagen IV. Although the tubes fused together along the degradable suture line, as designed, the leaflets shortened compared to their original height. This shortening is hypothesized to result from inadequate fusion at the commissures prior to suture degradation. With appropriate commissure reinforcement, this novel heart valve may provide the somatic growth potential desired for a pediatric valve replacement.

Keywords

heart valve; tissue engineering; congenital heart defects; matrix remodeling; pediatric

1.0 Introduction

The pulmonary valve is the heart valve most frequently afflicted by congenital heart defects, and there is a clinical need for a pulmonary valve replacement in pediatric patients. While this patient population is relatively small (~600/year in the U.S.),[14, 16] the need is dire because treatment can require multiple surgeries until adulthood to replace degenerated or

Robert T. Tranquillo (corresponding author), Department of Biomedical Engineering, 312 Church St SE, University of Minnesota, Minneapolis, MN 55455, Tel: 612-625-6868, Fax: 612-626-6583, tranquil@umn.edu.

outgrown valves.[11] Current replacement options for these children include glutaraldehyde-fixed xenografts, as well as decellularized or cryo-preserved homografts.[15, 19] Although there have been some improved preclinical and clinical outcomes,[3, 28] these valve replacement options traditionally have been prone to valve failure due to calcification, structural degeneration, and limited availability.[5] Additionally, these prosthetic valves are unable to grow with the patient and, consequentially, multiple valve replacements are often needed.[31]

Numerous tissue-engineered heart valve (TEHV) approaches have been explored that aim to produce a "living" valve capable of *in vivo* remodeling, repair, and ultimately somatic growth.[12] Although initially functional, most of these valves eventually failed due to leaflet shortening or fusion with the valve root, leading to an unacceptable level of regurgitation.[6, 7, 9, 20, 25] Most TEHV studies have utilized adult sheep, but studies with juvenile sheep have been reported.[9, 10] Two of these TEHVs contained cells at implant and ultimately failed due to leaflet shortening[9] and/or too much enlargement of the valve root.[10] Decellularization has been investigated as a way to reduce cell-mediated leaflet shortening and to increase their shelf-life.[6, 27, 30] Significantly, these approaches have demonstrated the feasibility of host cell invasion and matrix remodeling in both the pulmonary and aortic position.[6,24] However, long term function and growth of a TEHV has not yet been demonstrated.

Our group previously reported excellent hemodynamic performance of our decellularized TEHV in a pulse duplicator.[18] It is a tubular heart valve, comprised of two tubes of cell-produced matrix grown *in vitro* held together with degradable sutures.[18] These sutures are reported to maintain 50% of their initial strength after 4 weeks *in vivo*.[1] We have recently shown that single tubes implanted into young lambs as a pulmonary artery replacement with this suture exhibit somatic growth.[23] Thus, if the two tubes fuse with one another along the degrading suture line on that time scale by invading host cells, this valve should remain competent and possess growth potential.

The goal of this study was to evaluate the valve function and growth potential in a growing lamb model. Periodic ultrasounds were performed to evaluate valve function and growth before and after the expected time of suture degradation. Explanted valves were macroscopically, mechanically, histologically, and biochemically analyzed to assess tube fusion, recellularization, and new extracellular matrix deposition.

2.0 Materials and Methods

2.1 Tissue Fabrication

Tubular, cell-seeded fibrin gels were fabricated by mixing aqueous solutions of ovine dermal fibroblasts (ODFs, Coriell), bovine fibrinogen (Sigma), thrombin (Sigma), and calcium chloride. The final component concentrations were as follows: 1 million ODFs/mL, 4 mg/mL fibrinogen, 0.38 U/mL thrombin, and 5.0 mM Ca^{++}. The mixed solutions were injected into tubular glass molds which had a 19 mm inner diameter mandrel, a 4.5 mm annulus, and were ~9 cm in total length.

Following gelation, the tubular fibrin gels and glass mandrels were cultured in DMEM + 10% fetal bovine serum (FBS, Hyclone), 100 U/mL penicillin, 100 μg/mL streptomycin, 0.25 μg/mL amphotericin B,2 μg/mL insulin, and 50 μg/mL ascorbic acid. Culture medium was changed 3X per week for 2 weeks while allowing the longitudinal shortening of the gels. The tissue tubes were then removed from the glass rods and transferred onto 16 mm diameter latex tubes, which were attached to custom manifolds. Additional details on this pulsed-flow-stretch bioreactor have been previously reported.[26] Construct strain began at 3% and was incremented weekly by 1% until a 5% maximum strain was reached.

Following maturation, the engineered tubes were decellularized by immersion in 1% sodium dodecyl sulfate (SDS, Sigma) and 1% Triton X-100 (Sigma) for 6 hours and 30 minutes, respectively, at room temperature with continuous shaking. The tubes were then extensively rinsed in 1X phosphate buffered saline before and after overnight incubation in culture medium plus 2 U/mL deoxyribonuclease (Worthington Biochemical).

2.2 Valve Fabrication

Valves were fabricated using two 16 mm diameter engineered tubes, as previously described.[18] Briefly, the tubes were sutured together using 7-0 degradable sutures (Covidien Maxon CV) in 2 distinct patterns. The first suture line encompassed the entire circumference of the tubes and defined leaflet and commissure regions. A second suture line was added to reinforce each of the three commissure regions. On some valves, a single permanent suture (7-0 prolene) was then added to each commissure near the free edge.

2.3 Implantation Procedure in a Growing Lamb Model

The fabricated valves were implanted as pulmonary valve replacements in n=8 Dorset lambs (average age = 5.5 ± 0.8 weeks, average weight = 12.7 ± 0.5 kg). All protocols were approved by the Institutional Animal Care and Use Committee (IACUC) and performed by the University of Minnesota's Experimental Surgical Services. All animals were anesthetized using 10 mg/kg Ketamine and 2-6 mg/kg propofol and maintained on 2-4% isoflurane for the duration of the procedure. The heart was exposed via a left lateral thoracotomy with dissection through the intercostal space. Following surgery, animals received subcutaneous injections of 750IU heparin BID for the duration of the study. Animals were euthanized with beuthanasia given intravenously at 87-90 mg/kg.

Animals for the study were numbered as PACV1-8. The valves implanted in PACV1-2 did not utilize the single permanent sutures near the commissures, while PACV3-8 did. All tissue engineered valves were implanted interpositionally using 5-0 degradable sutures (Maxon CV, Covidien) in the main pulmonary artery after compromising the native pulmonary valve. A segment of the native pulmonary artery that matched the length of the implanted valve was also excised. Silver clips were attached on the ablumenal surface of the native pulmonary artery near the distal and proximal anastomoses to serve as markers (Figure 4a).

Valve function, flow velocity and profiles, pressure drop, and conduit dimensions were assessed from periodic transthoracic echocardiograms. The echocardiograms were first performed approximately 1 week after implantation and then monthly for the duration of the

study. Explanted valves were photographed and then dissected into strips for histological, biochemical, and mechanical characterization.

2.4 Tensile Mechanical Testing

Strips parallel ("circumferential") and orthogonal ("axial") to the circumference of engineered tubes and the native pulmonary artery were cut (~2 mm × 12 mm) and mechanically characterized using an Instron Biaxial tester. Strips were tested prior to implantation and after explantation. Strips were mounted in custom grips and straightened with a 0.005 N tensile load. Following 6 preconditioning cycles (0-10% strain), the samples were uniaxially strained to failure at 3 mm/min. Strain was calculated as the natural logarithm of the sample's deformed length divided by its initial length. Ultimate tensile stress (UTS) and modulus were defined as the maximum stress recorded and the slope of the linear region of the stress-strain curve, respectively. Representative stress-strain curves for the engineered tissue prior to and following implantation are shown in Supplemental Figure 1. Sample dimensions for calculating stress were measured using a digital caliper prior to testing.

2.5 Tissue Composition and DNA Quantification

The collagen mass content was determined using a hydroxyproline assay assuming 7.46 mg of collagen per 1 mg of hydroxyproline, as previously described.[22] Insoluble elastin was measured by dissolving the samples in NaOH and quantified using a modified ninhydrin assay.[21] The cell content was measured using a modified Hoechst assay for DNA assuming 7.6 pg of DNA per cell and reported as cell concentration.[13] Tissue volume for these tests was calculated using measured length, width, and thickness using a digital caliper.

2.6 Histology and Immunohistochemistry

Explanted valves were histologically and immunohistochemically stained using longitudinal strips that included the root, leaflets, and native pulmonary artery at each end. All samples were fixed in 4% paraformaldehyde, embedded in OCT (Tissue-Tek), frozen in liquid Nitrogen, and cut into 9 μm thick sections. Images were taken at 4×, 10×, or 20× magnification. Histological sections were stained with Lillie's trichrome, Verhoeff-Van Gieson, and Von Kossa stains. Immunohistochemical samples were blocked with 5% normal donkey serum, incubated in the primary antibody (2.5-5 μg/mL), and stained with a Cy5-conjugated, species-matched secondary antibody (Jackson Immunoresearch). Primary antibodies for this study included α-smooth muscle actin (α-SMA, Sigma, A5228), Von Willebrand Factor (vWF, Abcam ab6994), CD45 (US Biological C2399-07B), elastin (Abcam ab21599), and collagen IV (Abcam, ab6586). Nuclei were counterstained with Hoechst 33342 (Invitrogen H3570).

2.7 Statistics

Statistical significance was determined between two groups using Student's t-test and between multiple groups using ANOVA with a Games-Howell post-hoc test. Paired symbols in figures are used to represent statistical difference and a p-value < 0.05. All error bars are represented as the standard deviation of the group.

3.0 Results

3.1 Tissue Engineered Heart Valve

Completely biological heart valves (n=8, Figure 1a) were fabricated by sewing two decellularized engineered tubes together using 7-0 Maxon™ degradable sutures, as previously described.[18] The suture pattern was designed such that there were three commissures and three leaflets that collapse inward and close the valve when exposed to backpressure (Figure 1b), utilizing the principle of tubular heart valve design.[4] The engineered tubes used to make the valve consisted primarily of cell-produced collagen and other extracellular matrix proteins, although a residual fibrin layer remained on the lumenal surface following in vitro culture, as revealed by trichrome staining (Figure 1c).

Uniaxial strain-to-failure tests showed that the engineered tubes possessed an ultimate tensile strength (UTS) and modulus of 1.33 ± 0.16 MPa and 4.41 ± 0.82 MPa in the circumferential direction, respectively (Figure 1d,e). Mechanical tests in the orthogonal direction revealed that the engineered tubes were mechanically anisotropic, with the modulus being ~4 times stiffer in the circumferential direction. For comparison, mechanical testing was performed on excised native pulmonary valve leaflets and pulmonary artery (Figure 1d,e). The UTS and modulus of the engineered tissue were similar to values for the native pulmonary valve leaflets in both the circumferential and axial directions at the time of implant. The UTS and modulus of the native pulmonary artery were ~2.5 times lower compared to the engineered tissue values in the circumferential direction.

3.2 Valve Implantation

The valves were implanted into the main pulmonary artery of lambs (average weight = 12.7 ± 0.5 kg, average age = 5.5 ± 0.8 weeks) after resecting the native pulmonary valve leaflets and a length-matched section of the pulmonary artery (Figure 4a). The first two valves implanted contained only degradable sutures, while the subsequent 6 incorporated a single 7-0 prolene suture near the top of each commissure. The degradable suture line used to fabricate the valve and the anastomoses is visible in Figure 4a.

All animals survived the implant procedure and no perioperative deaths occurred, although three of the studies were ended prematurely. One animal did not recover well following surgery due to an atrial-septal defect. Two other valves were explanted due to inadequate initial valve function. In one animal, one leaflet was immobile immediately after implantation; the other animal developed extensive calcific nodules along the degradable suture line shortly after implantation. Since these studies were ended prematurely, and the purpose of this study was to assess long term valve function and remodeling, their outcomes will not be discussed further.

3.3 Valve Performance Evaluation with Ultrasound

Valve function and geometrical dimensions were assessed longitudinally using monthly ultrasounds (Figure 2). The first was performed 1.3 ± 0.3 weeks after implantation; full valve opening (Figure 2a) and closing (Figure 2b) were observed. Representative images at 8.1 ± 0.6 weeks (Figure 2c,d) and 21.1 weeks (Figure 2e,f) also demonstrated full leaflet

opening. Coaptation was adequate after 8 weeks (Figure 2d), but had decreased at the later time points based on regurgitant flow (Figure 2f).

All animals exhibited healthy weight gain over the course of the study (Figure 3a). In general, the insufficiency index increased over the duration of the study, particularly after the 8 week follow up time point (Figure 3b). A value of 1 on the insufficiency index indicates trivial regurgitation and higher values correlate to increased levels of regurgitation (2 = mild, 3 = moderate, 4 = severe). The diameter of the valves also increased over time (Figure 3c) and generally matched the neighboring pulmonary artery well. The mean and maximum (~1 week post implant = 11.6 ± 12.8 mmHg; ~16 weeks = 16.3 ± 11.0 mmHg) transvalvular pressure gradients also measured from the pulmonary valve velocity-time integral (PV VTI, Supplemental Figure 2).

The endpoint for each animal was dependent on animal health and overall valve function. Thus, the numbers of data points are not equal across all of the study time points; there are less data points at the later time points due to deteriorated valve function. The shortest and longest implantation periods included in the data quantification were 11.9 and 21.9 weeks, respectively. The other valves were explanted after 16.1, 19.1, and 19.4 weeks when adequate leaflet motion and coaptation was no longer apparent and the insufficiency index increased.

3.4 Explanted Valve Gross Pathology

At the endpoints, the explanted hearts and valves were analyzed to determine their integration and pathological abnormalities. Representative images of a valve at implant (Figure 4a) and explant (Figure 4b) are shown, with the clips demarcating the initial anastomoses, which became indistinguishable from the native pulmonary artery. All explanted valves were well integrated with the native pulmonary artery and excessive overgrowth or encapsulation was not present on the ablumenal surface (Figure 4b). The pre- and post-implant images are shown using the same scale to demonstrate the increase in root diameter and length during implantation. As observed at implantation (Figure 4a) and in subsequent ultrasounds, the valve diameter matched that of the surrounding native pulmonary artery well (Figure 4b). Further investigation of the heart revealed normal thickness and appearance of the right ventricle (Figure 4c).

The valves were excised from the pulmonary artery and cut longitudinally so that the lumenal surface could be visualized (Figure 4d). The lumenal surface was generally clean, although isolated nodules were present near one commissure on two of the five reported valves near the degradable suture line. As observed from the ablumenal surface, there was no clear anastomotic region; rather the native pulmonary artery and engineered root were seamlessly integrated. Importantly, there was also fusion along the original suture line between the two engineered tubes that formed the valve root and leaflets. However, the commissures were not stable relative to their position at implantation, indicated by the asterisks in Figure 4d. This instability allowed the leaflets to shorten by 43.3 ± 13.3% compared to their lengths at implantation (Figure 3d). In a two of the valves, this instability resulted in the complete disappearance of the leaflet. One inspected valve also exhibited some fusion from the leaflet belly towards the free edge. The remaining leaflets generally

were thin, pliable, and maintained the initial geometry prescribed by the suture pattern (Figure 4e).

3.5 Explanted Valve Mechanical Characterization

Strips cut from the explanted valve root, leaflet, and pulmonary artery were strained to failure to assess their tensile mechanical properties (Table 1). The thicknesses of the leaflet (0.58 ± 0.12 mm) and root (0.93 ± 0.12 mm) showed a reduction compared to the native pulmonary artery (1.30 ± 0.23 mm). The UTS and modulus in the circumferential direction were 1.75-4 times higher than the orthogonal (axial) direction. The circumferential UTS of the explanted valve root and leaflet were 1.27 ± 0.20 MPa and 2.54 ± 0.77, respectively, compared to the native pulmonary artery (0.28 ± 0.03 MPa). Additionally, strips incorporating both the pulmonary artery and root were taken in order to assess the strength of fusion and any influence of scar tissue at the anastomoses. UTS and modulus were comparable in the axial direction between these strips, the explanted valve root and leaflets, and native pulmonary artery (Table 1).

3.6 Explanted Valve Histological & Biochemical Analysis

Longitudinal strips were fixed, frozen, and included the proximal and distal pulmonary artery, root, and leaflet. The cross-sections in Figure 5 were taken from the middle of the leaflet free edge and stained with Lillie's trichrome, Von Kossa, and Verhoeff's stain. Following implantation, the leaflet and root tubes fused along the degradable suture line, as visualized in the trichrome image near this junction region (Figure 5a). Trichrome staining also revealed a cellular, collagenous matrix throughout the entire root and leaflet (Figure 5a-c). Immunostaining revealed Collagen IV deposition in the valve root and leaflets after 12 and 22 weeks (Figure 6e-h). Calcification was not observed in the engineered root or leaflets (Figure 5d-f), though small regions were observed near some anastomoses in proximity to the degraded sutures. Elastin was detected by immunostaining after 12 and 22 weeks in the root and leaflet sections (Figure 6a-d). Mature elastin can be detected using Verhoeff's stain and is manifested by black coloration (Figure 5g). Mature elastin was not observed in the leaflet sections (Figure 5h), but there were some mature fibers near the lumenal surface of the explanted root (Figure 5i).

Immunostaining was performed in order to identify the degree, location, and phenotypes of the invaded host cells at the shortest (~12 weeks) and longest (~22 weeks) time points. Complete recellularization of the root was observed at both time points as evidenced by the presence of nuclei (blue) throughout the entire length and thickness. Leaflet recellularization was sparser at both time points, although more nuclei were observed within the leaflets after 22 weeks. The majority of cells after 12 weeks, both within the root and on the leaflet surfaces, stained positive for α-SMA (Figure 6i,k). After 22 weeks, α-SMA was primarily expressed near the lumenal surface (indicated by the stars in Figure 6) of the root (Figure 6j) and partially on the leaflet surfaces (Figure 6l).

A complete endothelial layer, as evidenced by positive vWF staining, was observed on the lumenal surface of the root after both 12 and 22 weeks (Figure 6m,n). The leaflets were incompletely endothelialized after both 12 and 22 weeks (Figure 6o,p), though positive

staining was observed up to the leaflet free edge. Evidence of inflammatory and/or immune cells by CD45 expression was observed in the valves. CD45-positive cells were evident throughout the entire thickness of the root after 12 and 22 weeks (Figure 6q,r). Fewer CD45-positive cells were observed in the leaflets (Figure 6s,t). DNA quantification confirmed the presence of cells in the explanted engineered tissue, though not to the same degree as in the surrounding pulmonary artery (Table 2). The cell density in the explanted root was ~5.3 times higher compared to the leaflets (Table 2).

Collagen, elastin, and cellularity of the pre-implant tissue, explanted root, leaflet, and native pulmonary were quantified and compared (Table 2). Higher collagen and elastin density were observed following implantation compared to pre-implant tissue. Although higher than values at implantation, the elastin concentration in the engineered tissue was lower than that in the native pulmonary artery (Table 2). Prior to implantation, we previously reported a collagen concentration of 38 ± 4 mg/cm^3 for similar engineered tubes, which possessed negligible elastin content.[24] Total collagen content was estimated using the average collagen concentrations for the engineered root and leaflet regions. The total collagen was higher in the explanted root (81.2 ± 26.5 mg) compared to implant (49.1 ± 2.04 mg). The total collagen content in the leaflets was 15.2 ± 0.5 mg and 4.2 ± 1.8 mg before and after implantation, respectively.

4.0 Discussion

A pediatric heart valve capable of growth and remodeling has long been a goal of heart valve tissue engineering, but it has not yet been demonstrated. An ideal valve would be durable, hemocompatible, not prone to calcification, and possess the potential to grow with the patient. All of these characteristics functionally extend the life of a pediatric prosthetic valve and thus limit the need for subsequent surgeries to replace defective or outgrown valves. In light of this clinical need, we have developed a completely biological pediatric pulmonary valve using two decellularized, engineered tubes and degradable sutures. We previously reported the material and hemodynamic properties of these valves under simulated pulmonary valve conditions *in vitro*.[18]

Herein, we report the results of an *in vivo* study designed to assess long term valve function, tissue remodeling, and growth potential. All valves were implanted into the main pulmonary artery of lambs (average age = 5.5 ± 0.8 weeks) after excising the native pulmonary valve leaflets and a length-matched segment of the pulmonary artery. Although no perioperative deaths occurred, the implant procedure was refined over time. This included sewing the proximal anastomosis first and keeping the valve hydrated in order to better purge bubbles and avoid tissue sticking, respectively. The animals were evaluated monthly after implant using ultrasound until valve function deteriorated. The minimum and maximum implant durations of the 5 lambs studied were 11.9 and 21.9 weeks, respectively.

Overall, the valves performed well immediately and up to 8 weeks after implantation. This sustained function indicated that the critical process of fusion between the two engineered tubes had occurred along the degrading suture line given that it reportedly retains 50% of its original tensile strength after 4 weeks *in vivo*. However, valve function deteriorated

thereafter as evident from the insufficiency index (Figure 3b). The reasons for declining valve function are convoluted due to the fact that the root was enlarging (Figure 3c) and the sutures were further degraded and do not provide indefinite support. Thus, valve incompetence could arise from the enlargement of the root, without corresponding growth of the leaflets, or leaflet shortening due to inadequate fusion between the two tubes at the commissures prior to suture degradation.

Discerning between these two causes is complicated by animal growth, as Hoerstrup et al. also concluded.[10] In order to mitigate leaflet shortening, a single permanent suture was added to each commissure to provide long term support in these regions in the event that inadequate fusion was achieved. However, this approach did not prove successful (Figure 3d).

The engineered root diameter increased over time and matched the native pulmonary artery well, as observed from ultrasound. The engineered root diameter increased 126.3% from the first (age = 6.9 ± 1.0 weeks, weight = 15.3 ± 1.9 kg) to the last (age = 25.4 weeks, weight = 47.0 kg) echocardiogram. The lack of elevated mean and maximum transvalvular pressure gradients supports this observation (Supplemental Figure 2). In comparison, Gottlieb *et al.* studied the growth of the main pulmonary artery and reported an increase of only 31.4% for the pulmonary sinus diameter over the same weight range in Dorset sheep.[8] Interestingly, the percent increase in diameter of our TEHV root was comparable to the main pulmonary artery, as reported by Gottlieb et al., at earlier time points. The engineered root diameter increased only 6.9% and 18.2% from 1.4 to 4.3 and 8.0 weeks, respectively. Gottlieb *et al.* reported an increase of ~6.2% and ~12.8% in sheep between the same weight ranges.[8] The divergence of the increases in the diameter at longer time points is likely related to the elevated pulmonary insufficiency observed in the engineered valves at later time points. Pulmonary root dilation is known to result from pulmonary hypertension and abnormal hemodynamics, which are often byproducts of pulmonary insufficiency.[17] Notably, our group has previously reported somatic growth of a single engineered tube when implanted as a pulmonary artery replacement, without compromising the native pulmonary valve.[23]

After the valves became incompetent, they were explanted and subjected to macroscopic, mechanical, and histological analysis. There was no excessive overgrowth on the ablumenal surface of the valve and its diameter matched that of the surrounding vasculature, both of which were larger than at the time of implant (Figure 4a,b). The valves became integrated into the heart and were generally indistinguishable from the native pulmonary artery despite the degradation of the anastomotic sutures. Additionally, the two engineered tubes also fused along the degradable suture line and thereby formed leaflets *in situ* (Figure 4e). Significantly, tissue integration at the anastomoses appeared mechanically robust, based on their similar tensile failure mechanics compared to the surrounding tissue (Table 1).

Leaflet shortening (Figure 3d) was observed after implantation (Figure 4d), regardless of whether a permanent suture at the commissures was used or not. Since the leaflets were not extensively repopulated by α-SMA-positive cells, this shortening is likely due to commissure instability resulting from diastolic forces disrupting tissue fusion at the commissures. Leaflet fusion to the root from the belly region upwards, as reported by

Driessen-Mol *et al.*,[6] was only observed once in our study. Valve failure due to leaflet shortening has been reported previously, especially for pre-cellularized TEHVs.[6, 7, 9, 10, 25, 29] Gottlieb *et al.* reported elevated pulmonary insufficiency after 12 and 20 weeks.[9] They observed dimensional leaflet changes and reported that leaflet heights decreased by ~47% and 78.5% after implantation for 12 and 20 weeks, respectively. We observed shortening by 43.3 ± 13.3% compared to pre-implant values with no clear temporal dependence.

Recellularization is a crucial requirement for this approach, since the engineered tubes are acellular prior to valve fabrication and implantation. Although the integration of the tissue tubes along the degradable suture lines provide evidence of host cell invasion, more extensive characterization was necessary. Histology revealed uniform and complete recellularization throughout the engineered root and partial recellularization in the leaflet. Total cell number was quantified and was ~5.3 times higher in the engineer root compared to the leaflet (Table 2). Inflammatory and/or immune cells were observed by positive CD45 staining (Figure 6). It is expected that these cells would be absent after longer implantation times as seen in a study previously published by our group.[24] However the expected time scale is unknown since the current study was performed in a growing, as opposed to an adult animal. Other cell types present included endothelial cells on the surface and interstitial cells within the matrix. Driessen-Mol *et al.* reported similar recellularization patterns with their TEHV in adult sheep.[6] They also reported repopulation of endothelial and α-SMA positive cells in the root, and subsequently in the leaflets, over time. After 24 weeks, however, they reported that DNA content in their TEHV was similar to the native ovine valve leaflets, with homogeneous recellularization of the leaflets. In contrast, we observed cells primarily on the leaflet surfaces, but with an increasing number of cells within the leaflet matrix from 12 to 22 weeks of implantation.

In an attempt to distinguish between passive stretching and tissue growth, the total collagen content in the root and leaflets were compared before and after implantation. The total collagen content increased ~65% in the root while decreasing ~72% in the leaflets. The decrease in the leaflets is attributed to the decrease in leaflet height (and thus smaller volume) since the collagen concentration increased in both the root and leaflet regions (Table 2).[24] Histology revealed that the invading cells deposited elastin and collagen IV, which weren't present prior to implantation (Figure 6). The presence of the new matrix proteins, along with the maintenance of tissue mechanical properties (Figure 1d,e, Table 1), and the increase in total collagen in the root suggest that the invaded cells conferred true growth, not passive stretching of the engineered tube over time.

The recellularization pattern observed in this study contrasts with our observations from our aortic valve study in adult sheep. Previously, leaflet recellularization appeared to proceed with cells invading the base from the adjacent root and then migrating towards the leaflet free edge.[24] There were few cells present near the free edge even after 22 weeks.[24] In the present study, however, cells were observed on surface of the leaflets, including the free edge, as early as 12 weeks after implantation. These cells on were distributed fairly uniformly from the base to the free edge, with more cells invading from the leaflet surfaces at 22 weeks. These observations suggest that, in this study, the majority of cells repopulating

the leaflets originated from the blood instead of the adjacent root. However, we cannot discount the possibility that cells from the root very rapidly migrated over the surface and more slowly invaded from the surface.

We have demonstrated the *in vivo* function and remodeling of our decellularized TEHV in a growing lamb model after previously reporting its *in vitro* tissue and hemodynamic properties.[18] In this study, we observed fusion of the two engineered tubes along the degradable suture line, by design. The valves functioned well for the first 8 weeks, but pulmonary insufficiency increased over time due to the enlargement of the valve root and/or shortening of the leaflets. Extensive host cell invasion was observed following implantation in the engineered root, while the leaflets were partially recellularized. Importantly, host cell invasion and matrix remodeling occurred without large-scale calcification, although isolated regions were observed near the anastomoses.

Future studies will be needed to address the pulmonary insufficiency, the results demonstrate the feasibility of this approach to heart valve tissue engineering. One area that will be further explored relates to the most appropriate animal model to use since it grows much faster than in humans. The pulmonary artery grows at a rate of approximately 0.7 mm per year in humans[2] during childhood compared to approximately 8.5 mm per year in lambs.[8] Identifying a more suitable growth model will allow the recellularization process to occur on the time scale needed for the cells to respond to physiologic growth cues and allow for leaflet growth.

Supplementary Material

Refer to Web version on PubMed Central for supplementary material.

Acknowledgements

The authors acknowledge technical assistance from Sandy Johnson, Naomi Ferguson, Susan Saunders, the UMN Medical Devices Center, and the staff of the UMN Experimental Surgical Services and funding from NIH R01 HL107572 to R.T.T.

References

1. Maxon Monofilament Synthetic Absorbable Suture. 2008.
2. Akay HO, Ozmen CA, Bayrak AH, Senturk S, Katar S, Nazaroglu H, Taskesen M. Diameters of normal thoracic vascular structures in pediatric patients. Surgical and radiologic anatomy : SRA. 2009; 31:801–807. [PubMed: 19554251]
3. Cebotari S, Tudorache I, Ciubotaru A, Boethig D, Sarikouch S, Goerler A, Lichtenberg A, Cheptanaru E, Barnaciuc S, Cazacu A, Maliga O, Repin O, Maniuc L, Breymann T, Haverich A. Use of Fresh Decellularized Allografts for Pulmonary Valve Replacement May Reduce the Reoperation Rate in Children and Young Adults Early Report. Circulation. 2011; 124:S115–S123. [PubMed: 21911800]
4. Cox JL, Ad N, Myers K, Gharib M, Quijano RC. Tubular heart valves: a new tissue prosthesis design--preclinical evaluation of the 3F aortic bioprosthesis. The Journal of Thoracic and Cardiovascular Surgery. 2005; 130:520–527. [PubMed: 16077422]
5. Delmo Walter EM, de By TMMH, Meyer R, Hetzer R. The future of heart valve banking and of homografts: perspective from the Deutsches Herzzentrum Berlin. HSR proceedings in intensive care & cardiovascular anesthesia. 2012; 4:97–108. [PubMed: 23439605]

6. Driessen-Mol A, Emmert MY, Dijkman PE, Frese L, Sanders B, Weber B, Cesarovic N, Sidler M, Leenders J, Jenni R, Grunenfelder J, Falk V, Baaijens FP, Hoerstrup SP. Transcatheter implantation of homologous “off-the-shelf” tissue-engineered heart valves with self-repair capacity: long-term functionality and rapid in vivo remodeling in sheep. Journal of the American College of Cardiology. 2014; 63:1320–1329. [PubMed: 24361320]
7. Flanagan TC, Sachweh JS, Frese J, Schnoring H, Gronloh N, Koch S, Tolba RH, Schmitz-Rode T, Jockenhoevel S. In vivo remodeling and structural characterization of fibrin-based tissue-engineered heart valves in the adult sheep model. Tissue Engineering. Part A. 2009; 15:2965–2976. [PubMed: 19320544]
8. Gottlieb D, Fata B, Powell AJ, Cois CA, Annese D, Tandon K, Stetten G, Mayer JE Jr. Sacks MS. Pulmonary artery conduit in vivo dimensional requirements in a growing ovine model: comparisons with the ascending aorta. The Journal of Heart Valve Disease. 2013; 22:195–203. [PubMed: 23798208]
9. Gottlieb D, Kunal T, Emani S, Aikawa E, Brown DW, Powell AJ, Nedder A, Engelmayr GC Jr. Melero-Martin JM, Sacks MS, Mayer JE Jr. In vivo monitoring of function of autologous engineered pulmonary valve. The Journal of Thoracic and Cardiovascular Surgery. 2010; 139:723–731. [PubMed: 20176213]
10. Hoerstrup SP, Sodian R, Daebritz S, Wang J, Bacha EA, Martin DP, Moran AM, Guleserian KJ, Sperling JS, Kaushal S, Vacanti JP, Schoen FJ, Mayer JE Jr. Functional living trileaflet heart valves grown in vitro. Circulation. 2000; 102:III44–II49. [PubMed: 11082361]
11. Jacobs JP, Mavroudis C, Quintessenza JA, Chai PJ, Pasquali SK, Hill KD, Vricella LA, Jacobs ML, Dearani JA, Cameron D. Reoperations for pediatric and congenital heart disease: an analysis of the Society of Thoracic Surgeons (STS) congenital heart surgery database. Seminars in thoracic and cardiovascular surgery. Pediatric cardiac surgery annual. 2014; 17:2–8. [PubMed: 24725711]
12. Kheradvar A, Groves EM, Dasi LP, Alavi SH, Tranquillo R, Grande-Allen KJ, Simmons CA, Griffith B, Falahatpisheh A, Goergen CJ, Mofrad MR, Baaijens F, Little SH, Canic S. Emerging trends in heart valve engineering: Part I. Solutions for future. Annals of Biomedical Engineering. 2015; 43:833–843. [PubMed: 25488074]
13. Kim YJ, Sah RL, Doong JY, Grodzinsky AJ. Fluorometric assay of DNA in cartilage explants using Hoechst 33258. Analytical biochemistry. 1988; 174:168–176. [PubMed: 2464289]
14. Mozaffarian D, Benjamin EJ, Go AS, Arnett DK, Blaha MJ, Cushman M, de Ferranti S, Despres JP, Fullerton HJ, Howard VJ, Huffman MD, Judd SE, Kissela BM, Lackland DT, Lichtman JH, Lisabeth LD, Liu S, Mackey RH, Matchar DB, McGuire DK, Mohler ER 3rd, Moy CS, Muntner P, Mussolino ME, Nasir K, Neumar RW, Nichol G, Palaniappan L, Pandey DK, Reeves MJ, Rodriguez CJ, Sorlie PD, Stein J, Towfighi A, Turan TN, Virani SS, Willey JZ, Woo D, Yeh RW, Turner MB. Heart disease and stroke statistics--2015 update: a report from the American Heart Association. Circulation. 2015; 131:e29–322. [PubMed: 25520374]
15. Protopapas AD, Athanasiou T. Contegra conduit for reconstruction of the right ventricular outflow tract: a review of published early and mid-time results. Journal of cardiothoracic surgery. 2008; 3:62. [PubMed: 19017382]
16. Quality A. f. H. R. a. Healthcare Cost and Utilization Project (HCUP); 2014.
17. Raymond TE, Khabbaza JE, Yadav R, Tonelli AR. Significance of main pulmonary artery dilation on imaging studies. Annals of the American Thoracic Society. 2014; 11:1623–1632. [PubMed: 25406836]
18. Reimer JM, Syedain ZH, Haynie BH, Tranquillo RT. Pediatric tubular pulmonary heart valve from decellularized engineered tissue tubes. Biomaterials. 2015; 62:88–94. [PubMed: 26036175]
19. Ruzmetov M, Shah JJ, Geiss DM, Fortuna RS. Decellularized versus standard cryopreserved valve allografts for right ventricular outflow tract reconstruction: a single-institution comparison. The Journal of Thoracic and Cardiovascular Surgery. 2012; 143:543–549. [PubMed: 22340029]
20. Schmidt D, Dijkman PE, Driessen-Mol A, Stenger R, Mariani C, Puolakka A, Rissanen M, Deichmann T, Odermatt B, Weber B, Emmert MY, Zund G, Baaijens FPT, Hoerstrup SP. Minimally-Invasive Implantation of Living Tissue Engineered Heart Valves. Journal of the American College of Cardiology. 2010; 56:510–520. [PubMed: 20670763]
21. Starcher BC, Galione MJ. Purification and comparison of elastins from different animal species. Analytical biochemistry. 1976; 74:441–447. [PubMed: 822746]

22. Stegemann H, Stalder K. Determination of hydroxyproline. Clinica chimica acta; international journal of clinical chemistry. 1967; 18:267–273. [PubMed: 4864804]

23. Syedain, Z., Reimer, J., Lahti, M., Berry, J., Bianco, R., Tranquillo, R. 2015 4th TERMIS World Congress. Tissue Engineering Part A; Boston, MA: 2015. 50-Week Implant of a Tissue-Engineered Pulmonary Conduit in a Growing Lamb Model.; p. s-82.

24. Syedain Z, Reimer J, Schmidt J, Lahti M, Berry J, Bianco R, Tranquillo RT. 6-Month aortic valve implantation of an off-the-shelf tissue-engineered valve in sheep. Biomaterials. 2015; 73:175–184. [PubMed: 26409002]

25. Syedain ZH, Lahti MT, Johnson SL, Robinson PS, Ruth GR, Bianco RW, Tranquillo RT. Implantation of a Tissue-engineered Heart Valve from Human Fibroblasts Exhibiting Short Term Function in the Sheep Pulmonary Artery. Cardiovascular Engineering and Technology. 2011; 2:101–112.

26. Syedain ZH, Meier LA, Bjork JW, Lee A, Tranquillo RT. Implantable arterial grafts from human fibroblasts and fibrin using a multi-graft pulsed flow-stretch bioreactor with noninvasive strength monitoring. Biomaterials. 2011; 32:714–722. [PubMed: 20934214]

27. Syedain ZH, Meier LA, Reimer JM, Tranquillo RT. Tubular heart valves from decellularized engineered tissue. Annals of Biomedical Engineering. 2013; 41:2645–2654. [PubMed: 23897047]

28. Tudorache I, Cebotari S, Sturz G, Kirsch L, Hurschler C, Hilfiker A, Haverich A, Lichtenberg A. Tissue engineering of heart valves: biomechanical and morphological properties of decellularized heart valves. The Journal of Heart Valve Disease. 2007; 16:567–573. discussion 574. [PubMed: 17944130]

29. Weber B, Scherman J, Emmert MY, Gruenenfelder J, Verbeek R, Bracher M, Black M, Kortsmit J, Franz T, Schoenauer R, Baumgartner L, Brokopp C, Agarkova I, Wolint P, Zund G, Falk V, Zilla P, Hoerstrup SP. Injectable living marrow stromal cell-based autologous tissue engineered heart valves: first experiences with a one-step intervention in primates. European Heart Journal. 2011; 32:2830–2840. [PubMed: 21415068]

30. Weber M, Heta E, Moreira R, Gesche VN, Schermer T, Frese J, Jockenhoevel S, Mela P. Tissue-engineered fibrin-based heart valve with a tubular leaflet design. Tissue engineering. Part C, Methods. 2014; 20:265–275. [PubMed: 23829551]

31. Zubairi R, Malik S, Jaquiss RD, Imamura M, Gossett J, Morrow WR. Risk factors for prosthesis failure in pulmonary valve replacement. The Annals of Thoracic Surgery. 2011; 91:561–565. [PubMed: 21256315]

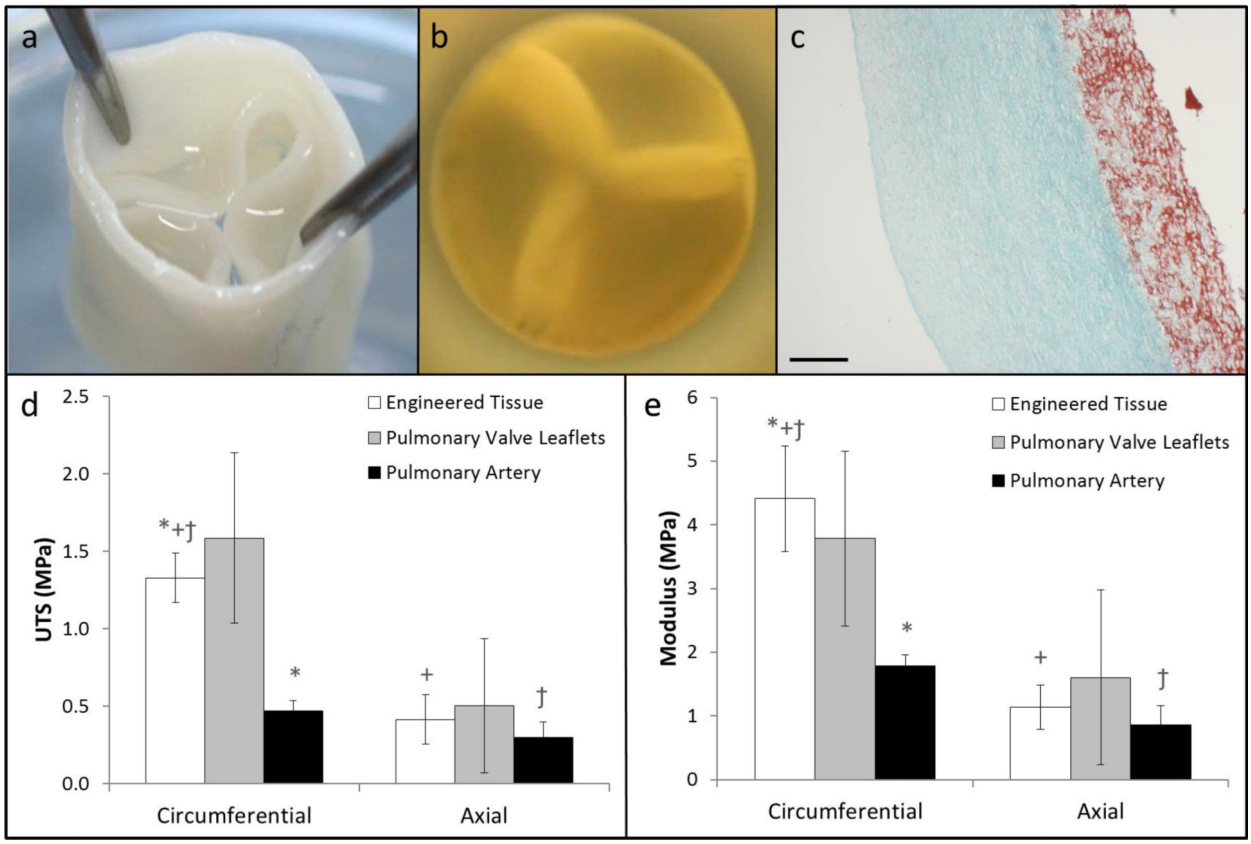

Figure 1.

Images of the tubular tissue-engineered valve (a) showing the leaflets, root, and (b) short axis view of the valve showing leaflet coaptation under physiologic backpressure. (c) Trichrome stained cross-section of the engineered tissue showing collagen (green) and non-collagen proteins (red); the scale bar is 250 μm. (d) Ultimate tensile strength and (e) tangent modulus of the engineered issue (n=4 for circumferential and axial), pulmonary valve leaflets (circumferential: n=3, axial: n=2), and the pulmonary artery (circumferential: n=4, axial: n=3) in the circumferential and axial directions at the time of implant. Paired symbols indicate a p-value < 0.05 between the two groups.

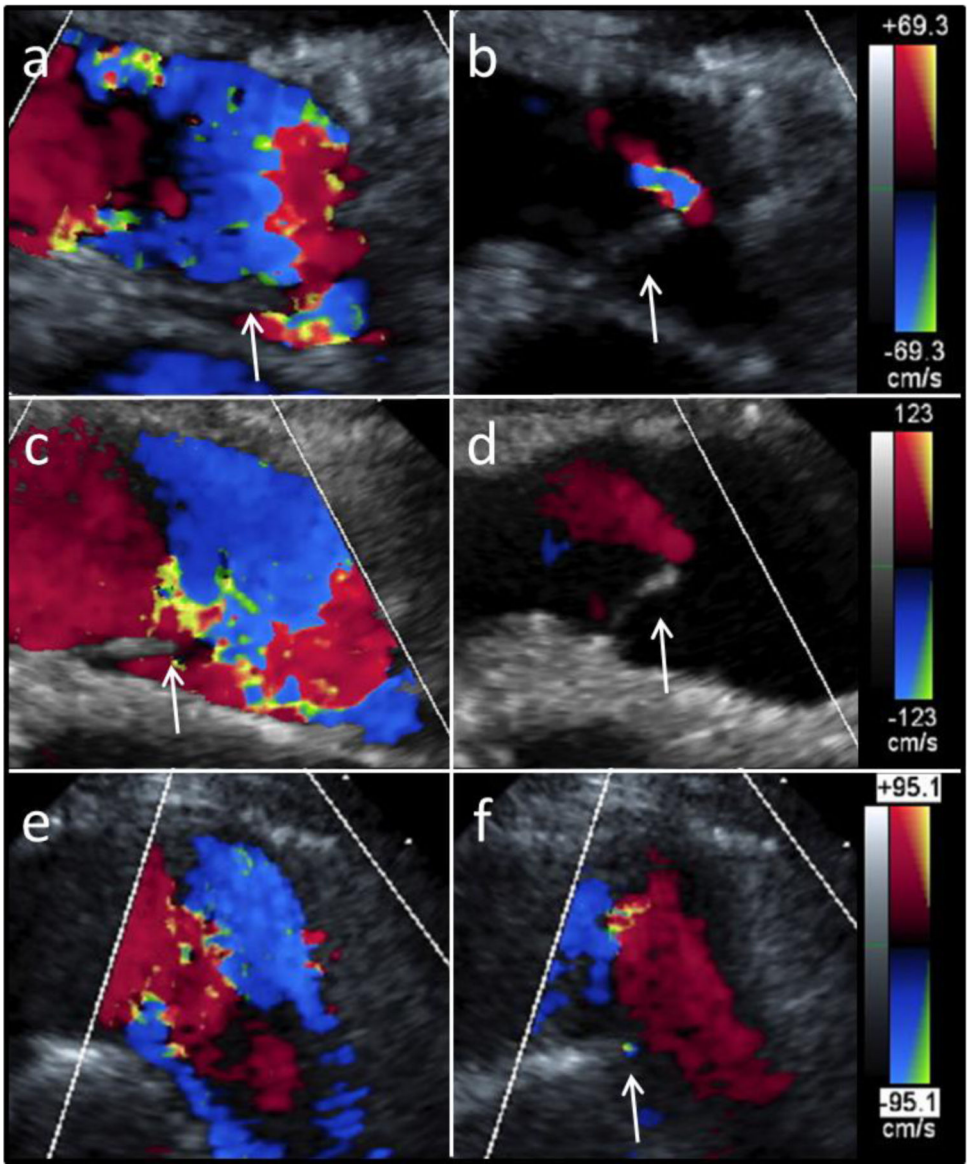

Figure 2.

Long axis ultrasound images of the valve (a,b) 1 week, (c,d) 8 weeks, and (e,f) 20 weeks after implantation. Representative images during (a, c, e) systole and (b, d, f) diastole show valve opening and closing, respectively. For all images, the right ventricle is on the left-hand side and the arrows point to the visible leaflets. Doppler scale bars for each time point are shown on the right.

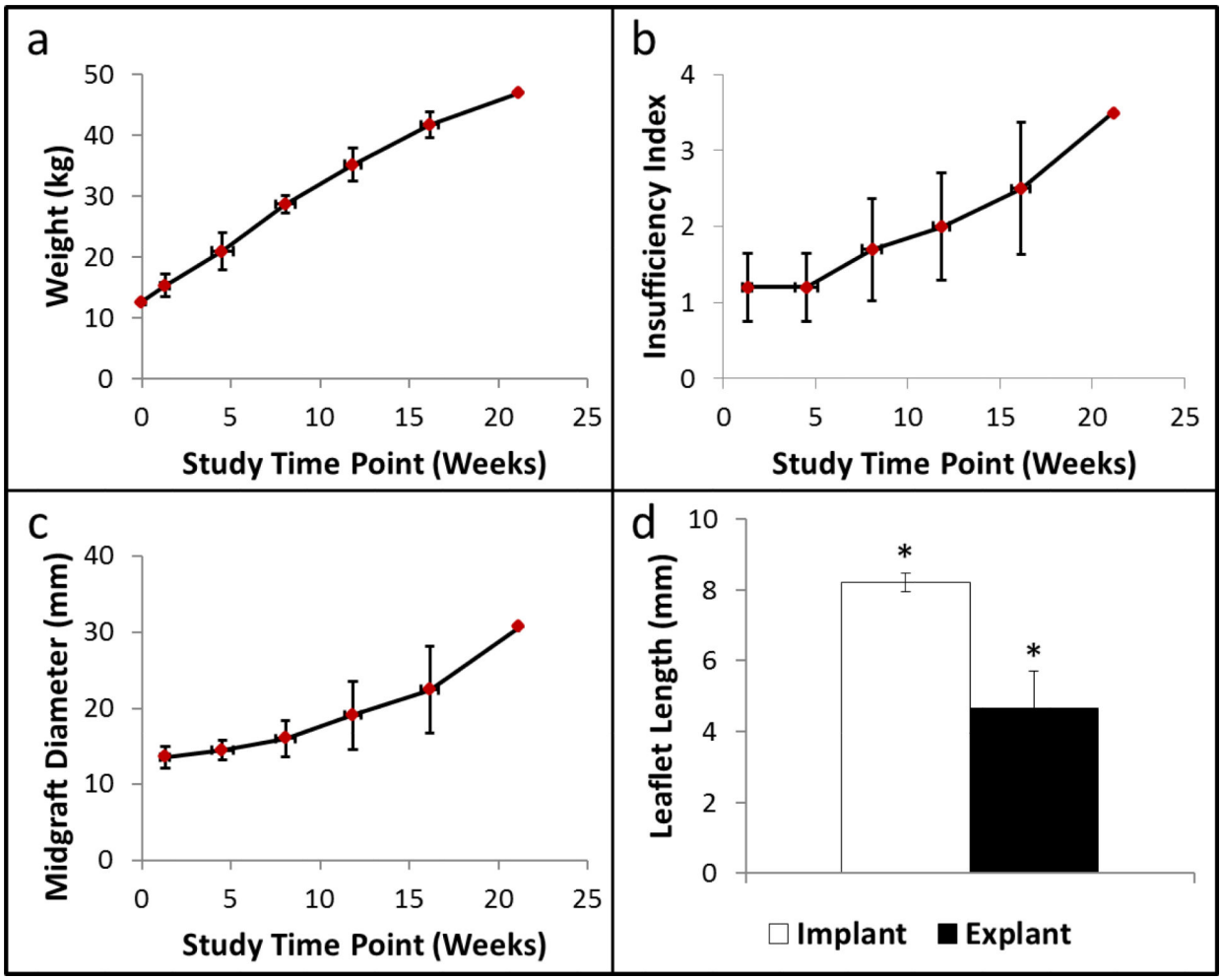

Figure 3.

(a) Animal weight, (b) valve insufficiency index, and (c) valve diameter midgraft as a function of study time point. (d) Leaflet length before and after implantation. N=5 for all panels. Paired symbols indicate a p-value < 0.05. Error bars in the x- and y-directions represent the standard deviation in the study time point and the measured values, respectively.

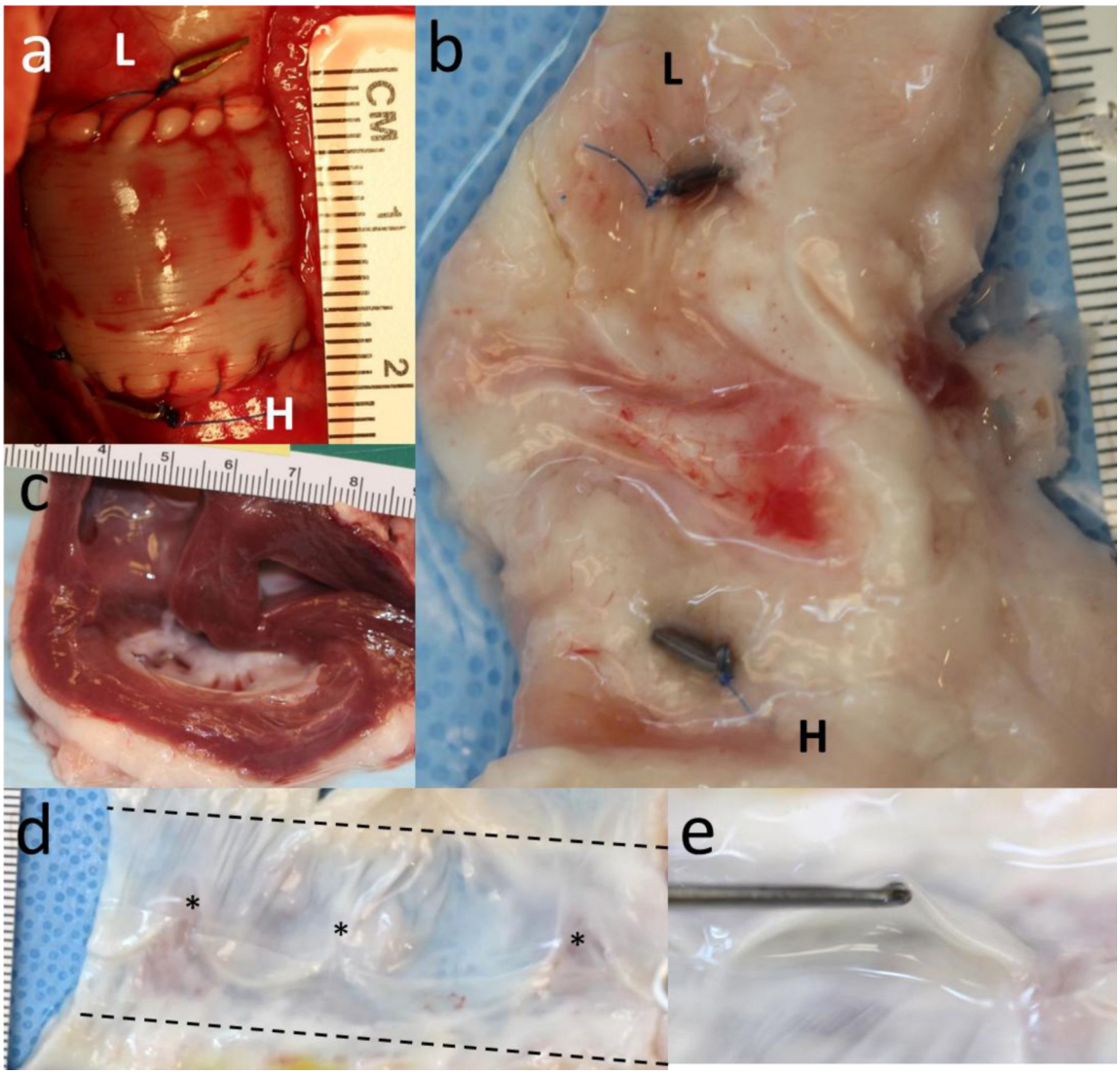

Figure 4.

Images of the valve (a) immediately after implantation and (b) explantation after 21.9 weeks at the same scale and in the same orientation. The “L” and “H” refer to the lung and heart end of the valve, respectively. In both images, the clips are visible on the ablumenal surface of the native pulmonary artery. (c) Cross-section of the heart showing normal right ventricle thickness after 21.9 weeks. (d) An explanted valve cut open to show its lumenal surface and leaflets. Stars indicate the original position of the commissures. (e) End-on view of a leaflet.

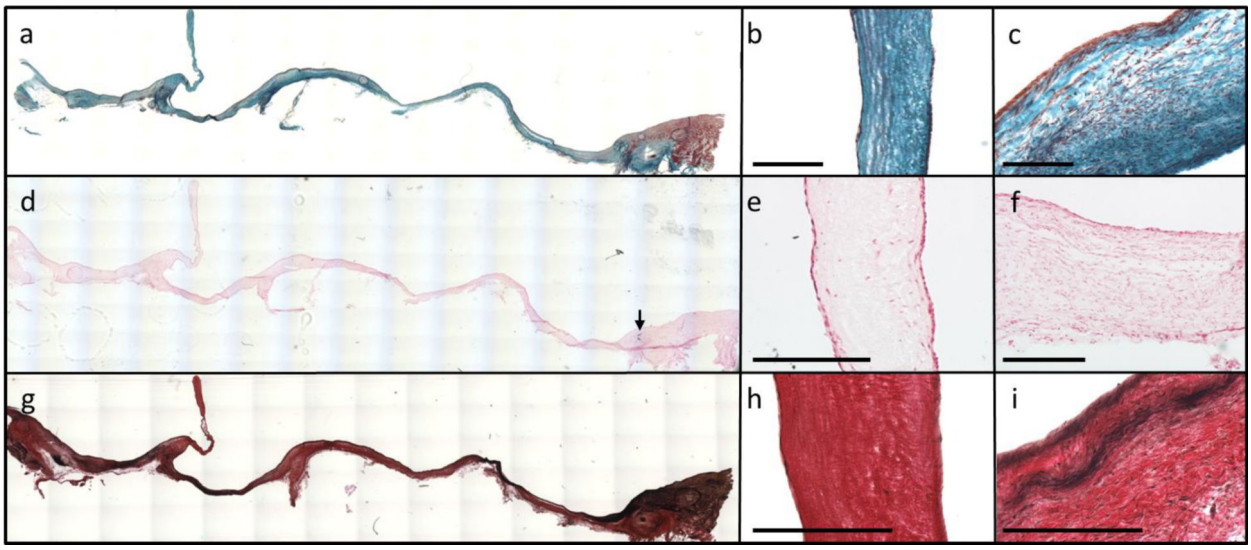

Figure 5.

Reconstructed cross-sectional images of the explanted valves (a, d, g) with the proximal side on the left and the distal side on the right. (a) Trichrome staining revealed collagen (green) throughout the entire valve (b) leaflet and (c) root. (d) Von Kossa staining revealed no apparent calcification in the valve (e) leaflet and (f) root, except near some of the degradable sutures where calcific nodules formed in three animals. Arrow points to calcification present near anastomosis in the pulmonary artery (g) Verhoeff staining to detect mature elastin (black) in the valve (h) leaflets and (i) root. Scale bars for all images are 250 μm.

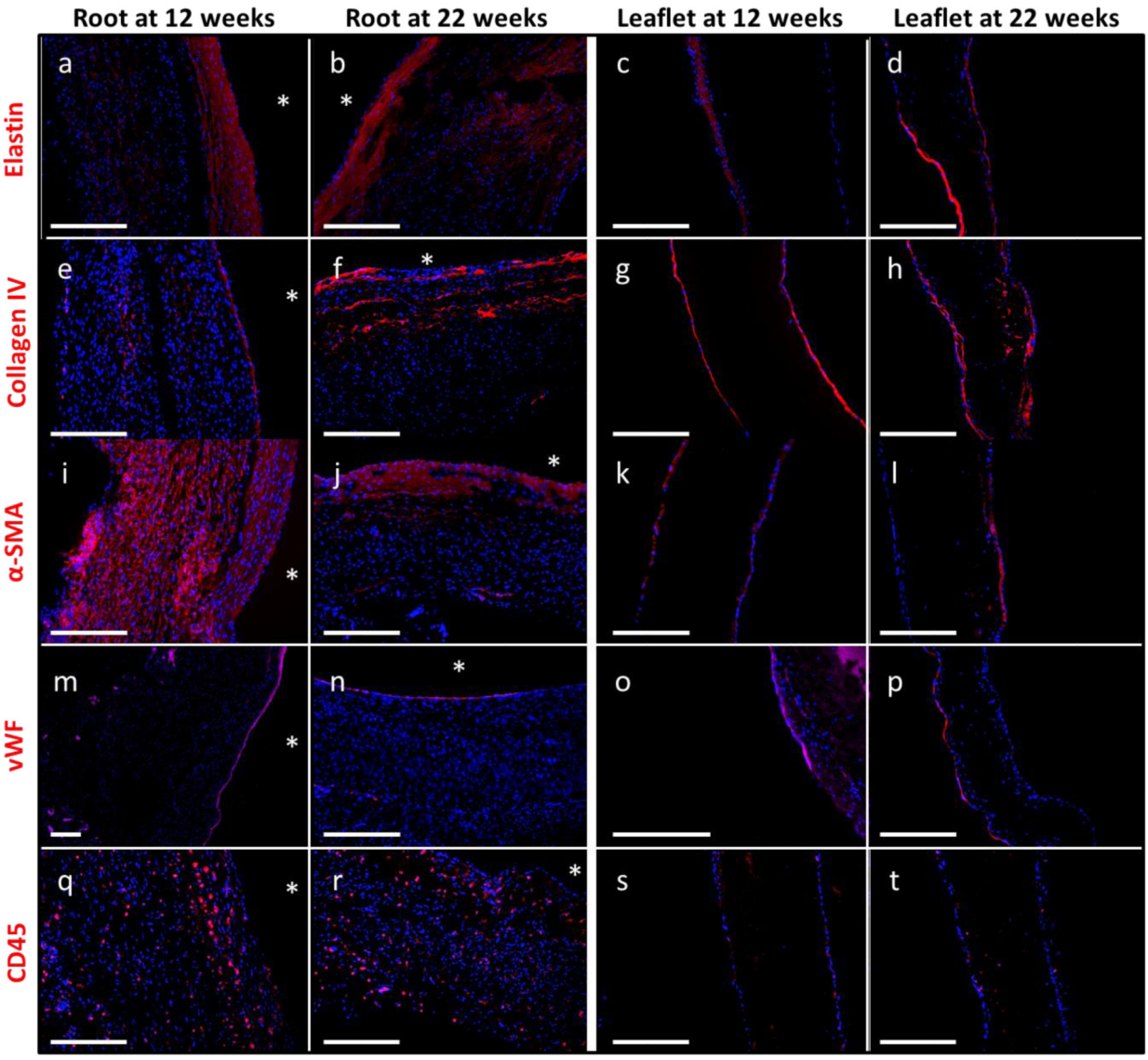

Figure 6.

Comparison of cell markers and matrix proteins in the valve root and leaflet after implantation for 12 or 22 weeks. Cell markers included (a-d) α-SMA, (e-h) vWF, and (i-l) CD45. Immunostaining for matrix proteins revealed the presence of (m-p) elastin and (q-t) collagen IV in the valve root and leaflets. All primary antibodies are pseudo-colored in red and counterstained with Hoechst to visualize cell nuclei. Asterisks indicate the lumenal surface of the valve root.

Table 1

Tensile mechanical properties of the explanted engineered root, leaflets, native pulmonary artery, and anastomoses

Sample Description	Sample Orientation	Thickness (mm)	UTS (MPA)	Modulus (MPA)
Explant Root	**Circumferential Axial**	0.93 ± 0.12	1.27 ± 0.20 0.68 ± 0.27	4.11 ± 1.76 2.32 ± 1.06
Explant Leaflet	**Circumferential Axial**	0.58 ± 0.12	2.54 ± 0.77 0.87 ± 0.28	7.93 ± 2.71 1.94 ± 0.92
Anastomosis	**Axial**	1.59 ± 0.14	0.48 ± 0.29	1.43 ± 0.90
Native Pulmonary Artery	**Circumferential Axial**	1.30 ± 0.23	0.28 ± 0.03 0.24 ± 0.12	0.93 ± 0.34 0.64 ± 0.30

Table 2

Biochemical properties and DNA concentration of the explanted engineered root, leaflets, and native pulmonary artery

Property	Explanted Root	Explanted Leaflet	Pulmonary Artery
Total Collagen (mg/mL)	63.0 ± 23.7	56.8 ± 15.2	20.5 ± 8.6
Elastin (mg/mL)	9.9 ± 5.0	1.6 ± 0.8	19.6 ± 12.1
Cellularity (Million cells/mL)	170.2 ± 37.0	31.9 ± 25.2	297.9 ± 109.6